

# In situ solid-state NMR studies of $\text{Ca}_3\text{SiO}_5$ : hydration at room temperature and at elevated temperatures using $^{29}\text{Si}$ enrichment

A. R. BROUGH, C. M. DOBSON

*Inorganic Chemistry Laboratory, University of Oxford, South Parks Road, Oxford, OX1 3QR, UK*

I. G. RICHARDSON, G. W. GROVES

*Department of Materials, University of Oxford, Parks Road, Oxford, OX1 3PH, UK*

$^{29}\text{Si}$  isotopic enrichment was used for acquisition of multiple  $^{29}\text{Si}$  magic-angle spinning (MAS) and cross-polarization magic-angle spinning (CPMAS) nuclear magnetic resonance (NMR) spectra, *in situ* in an NMR probe, from a single sample of hydrating  $\text{Ca}_3\text{SiO}_5$  ( $\text{C}_3\text{S}$ ). Data with excellent signal-to-noise ratios were obtained at 20, 50 and 75 °C, with minimal use of spectrometer time, and without the need for the quenching of multiple samples. Spectral line widths and polymer-chain lengths derived from the spectra had no detectable differences from experiments in which the quenching was carried out with propan-2-ol. Furthermore, the effects of the MAS technique on the hydration reaction appeared to be minimal. At 20 °C, the bulk hydrate initially produced was dimeric; at later stages of the reaction, polymerization occurred. Arrhenius energies of 35 and 100  $\text{kJ mol}^{-1}$ , respectively, were calculated for these two reactions. The cross-polarization (CP) spectra acquired throughout the hydration showed that at 20 °C, 2% of the hydrated monomeric  $\text{Q}_0^{(\text{H})}$  species persisted from after the induction period through to the late stages of the hydration reaction; this indicates that this species is unlikely to result from surface hydroxylation of  $\text{C}_3\text{S}$ ; an upfield shift of this species occurred with increasing hydration, indicating a possible change of environment for the silicate species. The amount of  $\text{Q}_0^{(\text{H})}$  produced was found to increase at higher temperatures. Potential mechanisms for polymerization were assessed and a model in which dimeric-silicate units are linked together by insertion of monomers (dimer  $\rightarrow$  pentamer  $\rightarrow$  octomer) was found to give the best fit to the observed data; these results support a dreierketten model for the structure of the hydrate.

## 1. Introduction

The calcium-silicate hydrate (C–S–H) gel (Cement chemists notation,  $\text{C}=\text{CaO}$ ,  $\text{S}=\text{SiO}_2$ ,  $\text{H}=\text{H}_2\text{O}$ , for example,  $\text{C}_3\text{S}=\text{Ca}_3\text{SiO}_5$ ) that forms as the major product of ordinary Portland cement (OPC) hydration is difficult to characterize. A wide range of techniques has been used to investigate the structure of the crystalline components of OPC, the reactions that occur during hydration, and the products that are formed. Diffraction studies have proved useful for characterizing the components of anhydrous OPCs, but they are of limited use in the study of the C–S–H gel which forms upon hydration, because of its limited crystallinity and the presence of other hydration products. Studies of synthetic C–S–H gels with higher crystallinities suggest that their structures may be related to that of 1.4 nm Tobermorite or to Jennite; a number of models for the structure of C–S–H based upon this assumption have been proposed in the literature [1, 2, 3]. The phases present in the hydrated material can be quantified by the use of thermo-

gravimetric techniques. The structure of the silicate species in the gel, and in the pore solution, can be determined by chemical methods; for example, reaction of the gel with tetramethylsilylchloride, and analysis of the products by chromatography, can determine the nature of the silicate species which were originally present [4, 5, 6, 7]. Colorimetric methods are also available [8]. Care is needed in the interpretation of the results, since there is a possibility that, under the severe conditions required to achieve derivatization of the silicate anions in the C–S–H gel, rearrangement may take place. The morphology and composition of the phases contained within hydrated gels can be studied by transmission electron microscopy (TEM) of ion-beam-thinned samples [9, 10].

Another technique available to cement chemists is  $^{29}\text{Si}$  solid-state nuclear magnetic resonance (NMR). This technique is sensitive to the *local* co-ordination of the silicate species, and it enables the gel to be studied *without* chemical manipulation. It is possible to obtain spectra from static samples, but very rapid spinning of

samples is necessary to average the anisotropy of the chemical shift. Such rapid magic-angle spinning (MAS) allows the various silicate species to be resolved; each of the five  $Q_n$  species (in the  $Q_n$  notation ( $0 \leq n \leq 4$ ),  $Q$  is a silicate tetrahedra, and  $n$  is the number of oxygens which bridge to adjacent silicate tetrahedra) has been found, empirically, to have a characteristic chemical-shift range. Note that while it is possible from measurements of the relative intensities of the  $Q_n$  peaks to obtain information with regard, for example, to *average* chain lengths; it is not possible to determine the *absolute* chain lengths. Solid-state NMR is only affected to a limited degree by the lack of long-range order; poorly crystalline materials have larger line widths, and spectra from these materials are more difficult to resolve. Resolution can also be degraded severely in materials or mixtures which contain paramagnetic species [11].

There is a large body of literature in which cements and related materials have been studied by solid-state NMR. Many of these studies related to  $C_3S$ , which can be used as a model for OPC, with the advantage that the NMR spectra acquired from hydrated  $C_3S$  have significantly better resolutions than the spectra acquired from hydrated OPC. After an initial study of a range of crystalline silicates of known structures [12], two studies of  $C_3S$  hydration [13, 14] showed that the calcium-silicate-hydrate gel formed contains only  $Q_1$  and  $Q_2$  species; no evidence was found for the formation of more highly polymerized species. Numerous studies have followed, and it has been shown that essentially the same results are obtained for the hydration of OPC [15] and  $\beta$ - $C_2S$  [16, 17]. Gels formed from all these materials also have the same chemical composition, with a Ca:Si ratio of approximately 1.7 [9, 18]; additional Ca is deposited as CH. These results show that  $^{29}Si$  MAS NMR is a valuable technique for the study of the hydration both of OPC and of  $C_3S$ , its principal silicate-containing component, and they indicate that  $C_3S$  can be used as a good working model for OPC.

Many of the previous studies of C-S-H gels by NMR obtained spectra from quenched gels. The hydration reaction is quenched in such studies by the addition of a solvent such as propan-2-ol, followed by outgassing under vacuum. While the effects of humidity during long-term curing have been studied [19], it is unclear what effect *rapid* quenching may have upon the structure of C-S-H gels. In order to investigate early C-S-H gels without quenching, it is necessary to acquire NMR spectra very rapidly, as the gels are formed. It would normally take a significant time to obtain spectra with good signal-to-noise ratios, but  $^{29}Si$  enrichment can be used to enable the acquisition of spectra more rapidly. In order to obtain these *in-situ* spectra, it is necessary to subject the hydrating gels to MAS, which might be expected to impose large forces upon the sample; hence we also have to investigate the effects of MAS upon the hydration reaction. In this paper, we describe studies of  $C_3S$  hydration with  $^{29}Si$ -enriched reagents, including experiments which were performed to determine the effects of quenching upon the spectra obtained from hydrated-cement gels,

and to determine the effects of MAS upon the hydration reaction.

An area of current interest is the behaviour of cementitious systems at elevated temperatures, such as are found, for example, in oil wells, and after back-filling of radioactive-waste depositaries. While there is much literature concerning the investigation of the crystalline products produced by cement hydration at very high temperatures and pressures, less work has been performed under more moderate conditions. Recently, the hydration of  $C_3S$  and of a class G cement has been studied by  $^{29}Si$  NMR over the temperature range 60–120 °C [20]; the rate of reaction and the degree of polymerization attained by the gel have been shown to increase with temperature. Similar results have been obtained from materials hydrated as mortars or concretes [21, 22]. These spectra, in which  $C_3S$  containing  $^{29}Si$  at its natural abundance was generally used, are insufficient for a full kinetic analysis of the reactions to be carried out. These results also appear to show the production of very large quantities of  $Q_0^{(H)}$  species (see below) at the highest temperatures. Previously, heat-evolution data [23, 24] for the early stages of hydration have been fitted to the Avrami equation [25], and activation energies in the range 80–120 kJ mol<sup>-1</sup> have been obtained from the temperature dependence of the calculated reaction rates.

In this paper we describe a detailed study, by  $^{29}Si$  NMR, of the hydration of  $C_3S$  at the temperatures, 20, 50 and 75 °C. A separate sample hydrated at 80 °C was also studied by TEM in order to determine the effects of hydration upon the microstructure of the hydrate at this elevated temperature. Additionally, we acquired  $^{29}Si$  CPMAS spectra, with excellent signal-to-noise ratios throughout the later stages of the hydration reaction, for the hydration of  $C_3S$  at both 20 and 75 °C. The  $Q_0$  region (–68 to –76 p.p.m. (parts per million)) of the MAS NMR spectrum of hydrating systems was obscured by a signal from residual anhydrous material: the technique of cross polarization (CP) [26, 27] can, however, be used to observe only those resonances resulting from hydrated material [14]. Magnetization is generated by excitation of  $^1H$  nuclei, and it is then transferred to the  $^{29}Si$  nuclei by a mixing, or contact, pulse; only those  $^{29}Si$  species which are close to protons on a nanometre scale are observed. It has been possible to observe hydrated monomeric  $Q_0^{(H)}$ -silicate species; such species are produced during the induction period, and attention has been focused on this phase of the hydration reaction, and on the period immediately after it [28]. It has been postulated that, thereafter, the  $Q_0^{(H)}$  species decays with time, suggesting that this species may result from surface hydroxylation of  $C_3S$  [29]. The intensity of the peaks in the CP spectra cannot, however, be directly related to the concentrations of the species giving rise to them; the intensity of a particular resonance depends upon both the duration of the contact pulse, and the relaxation properties of the nuclei studied. The dynamics of this process can be examined by obtaining spectra at a range of contact times; we have acquired such series of spectra, with the aim of aiding the quantification of the  $Q_0^{(H)}$  resonance. Such quantification of the various

silicate species during the course of  $C_3S$  hydration at a range of temperatures should assist in discriminating between the various models for the structure of calcium-silicate hydrate, and for the mechanism of  $C_3S$  hydration.

## 2. Experimental procedure

$^{29}\text{Si}$  NMR spectra were acquired at a resonant frequency of 39.76 MHz by the use of a Bruker MSL200 spectrometer with a 4.7 T magnet. Spectra were acquired with MAS at 1–3 kHz in a double-bearing CPMAS probe, from samples packed into 7 mm zirconia rotors, with  $^1\text{H}$  decoupling at a field strength of approximately 60 kHz. The probe was shimmed by observation of the  $^{13}\text{C}$  CPMAS spectrum of adamantane. The magic angle was set by observation of the  $^{79}\text{Br}$  resonance from KBr.  $^{29}\text{Si}$  chemical shifts were referenced to tetra methyl silane (TMS) at 0 p.p.m., by the use of kaolinite as an external reference (chemical shift  $-91.2$  p.p.m. [30]), or by use of residual  $C_3S$  as an internal reference. For  $^1\text{H}$ - $^{29}\text{Si}$  CP, the Hartman-Hahn match was set by maximization of the signal from kaolinite, except for samples where the signal-to-noise ratio was sufficiently good that the match could be set using the sample. Quantification of resonances in the CP spectra was achieved without an external reference by comparison with the intensities in the single-pulse spectra; this procedure is described in more detail later in this paper. Unless indicated otherwise, for the CP spectra, 1024 data points were acquired at a sweep width of 7042 Hz, apodized with 10 Hz of Lorentzian line broadening, and zero filled to 8192 points prior to Fourier transformation. For single-pulse spectra, 1024 data points were acquired at a sweep width of 7042 Hz, apodized with 5 Hz of Lorentzian line broadening, and zero filled to 8192 points prior to Fourier transformation.

Samples for the real-time study of hydration were prepared from demineralized water and  $C_3S$  enriched in  $^{29}\text{Si}$  to 100%; a water-to-solids ratio of 0.5 was used. The  $^{29}\text{Si}$ -enriched  $C_3S$  was prepared by repeatedly firing a stoichiometric mixture of  $\text{Ca}(\text{OH})_2$  and  $^{29}\text{SiO}_2$ . The samples for hydration were mixed in small rotor inserts made from delrin with push-fit lids, and they were sealed with a fast-setting epoxy resin to permit MAS. Problems were experienced with sealing the inserts; if the lids were simply forced on, then the excess pressure generated inside the inserts caused liquid to escape before the epoxy resin had time to set. It proved necessary to drill small vent holes in the lids; the dry powders were then placed in the inserts and premixed; the appropriate amount of water was then added, and the samples were vigorously mixed for 5 min. The lids were put in place, and sealed with epoxy resin. Additional epoxy resin was then used to seal the small vent holes in the lids, and the delrin inserts were loaded into 7 mm zirconia rotors and placed in the NMR probe. The temperature was set to the required value, and hydration was allowed to proceed until the cement paste had begun to set. The samples were then subjected to MAS at approximately 1.5 kHz to enable acquisition of the NMR spectra.

Hence, for each sample, the first spectrum acquired corresponded to the point in time at which the sample was first subjected to MAS. As the hydration proceeded, it was necessary to adjust the tuning of the NMR probe at frequent intervals. The spectra were acquired continuously over a period of approximately 4 days, during which time the samples were subjected to MAS. Thereafter, spectra were acquired intermittently, and the samples were subjected to MAS for the duration of these periods of acquisition only; during the intermediate periods, the sealed sample containers were stored under moist conditions at the appropriate temperature. Elevated temperatures were achieved by heating the gas supply to the MAS turbine bearings; it is estimated that temperatures were accurate to  $\pm 5^\circ\text{C}$ , and stable to  $\pm 2^\circ\text{C}$ . The techniques used for control and calibration of the temperature have been described elsewhere [31].

Integration of single-pulse spectra was performed using the Bruker proprietary spectrometer software (DISMSL), after careful manual correction of baselines by subtraction of a fifth-order polynomial. The CPMAS spectra were iteratively fitted to Voigt line shapes using the software package IGOR [32], running upon an Apple Macintosh computer: a fourth-order polynomial baseline correction was also made.

## 3. Results

### 3.1. $^{29}\text{Si}$ MAS NMR spectra

$^{29}\text{Si}$  MAS NMR spectra were acquired from samples of  $C_3S$  hydrated at three temperatures:  $20^\circ\text{C}$ ,  $50^\circ\text{C}$  and  $75^\circ\text{C}$ . Two samples were independently hydrated at  $20^\circ\text{C}$ , and three samples were hydrated at  $75^\circ\text{C}$  in order to determine the reproducibility of the data. One of the samples hydrated at  $75^\circ\text{C}$  was quenched after partial hydration, in order to determine the effects of quenching upon the silicate polymerization. Additionally a further sample was hydrated under static conditions at  $80^\circ\text{C}$ .

Representative series of the single-pulse spectra acquired from these samples hydrated at 20, 50, and  $75^\circ\text{C}$  are shown in Fig. 1. In each case, the following were observed:  $Q_0$  resonances ( $-65$  to  $-75$  p.p.m.) which results from anhydrous  $C_3S$  resonances from chain-end  $Q_1$ -silicate species ( $-79$  p.p.m.), and resonances from middle-chain  $Q_2$ -silicate species ( $-85$  p.p.m.). In no case were more highly polymerized ( $Q_3$  or  $Q_4$ ) silicate species observed. For each series of MAS spectra, the line widths of the group of  $Q_0$  resonances from  $C_3S$  were narrow and remained constant throughout the course of the hydration reaction, and at the different temperatures. The relative intensities within this group of resonances were found not to change; their overall intensity, however, decreased with time. The line widths of the  $C_3S$  and C-S-H resonances were not found to be significantly increased in the  $^{29}\text{Si}$ -enriched samples relative to the line widths observed in samples which contained  $^{29}\text{Si}$  at its natural abundance; this indicates that homonuclear dipolar coupling was not a significant contribution to the line widths. The line widths of the  $Q_1$  and  $Q_2$  resonances were, however, considerably larger

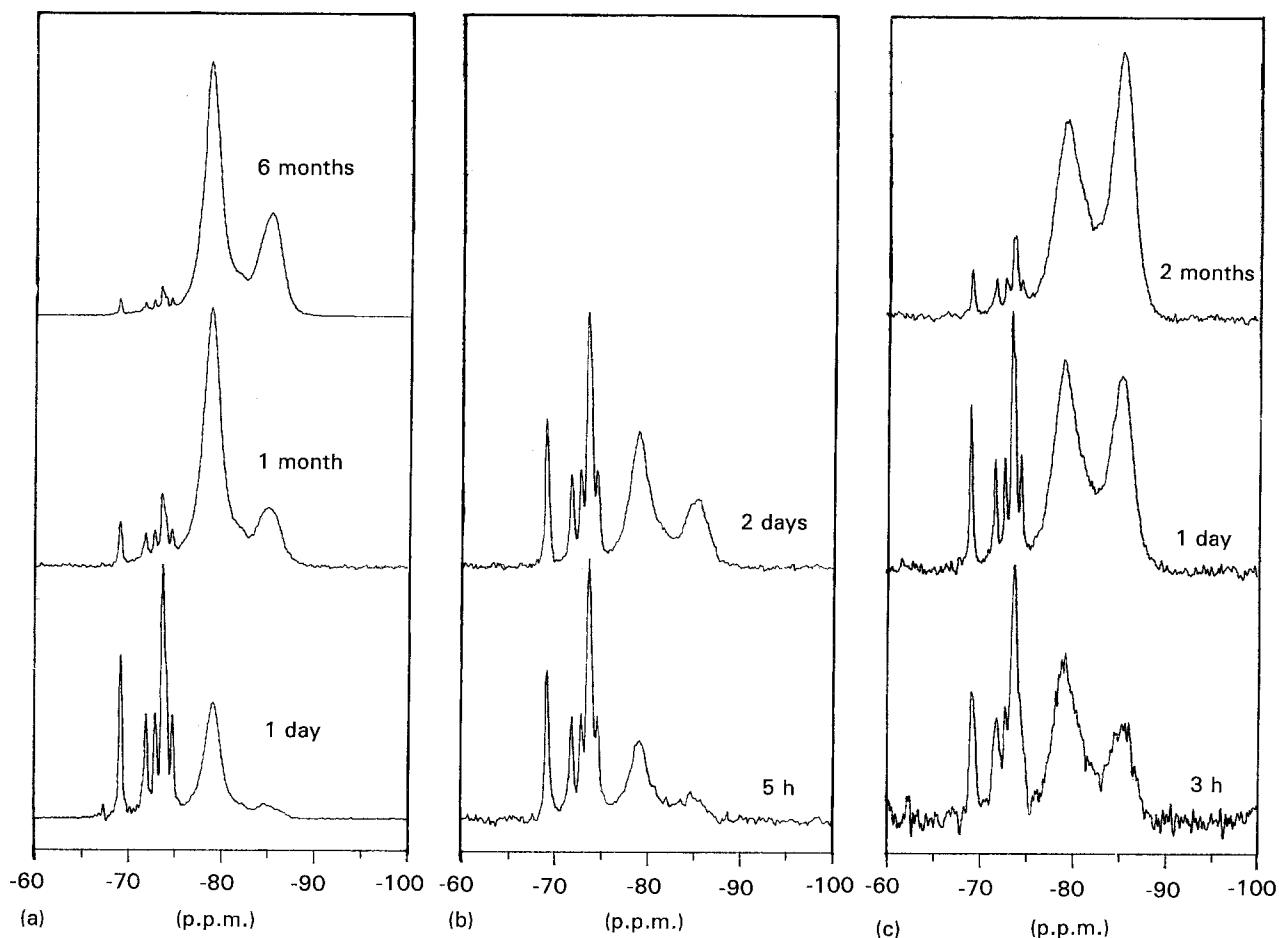


Figure 1 Representative  $^{29}\text{Si}$  MAS NMR spectra of  $\text{C}_3\text{S}$  samples hydrated at a water-to-solids ratio of 0.5, and temperatures of: (a)  $20^\circ\text{C}$ , (b)  $50^\circ\text{C}$ , and (c)  $75^\circ\text{C}$ . The isotropic peaks are labelled with the  $Q_n$  assignments. Only a very small fraction of the total number of spectra acquired from each sample are shown.

than those of the anhydrous  $Q_0$  resonances; this is attributable to the fact that the  $Q_0$  resonances result from crystalline material, whereas the  $Q_1$  and  $Q_2$  resonances result from the amorphous hydrated gel.

At each temperature,  $Q_1$  species were the major products of the early stages of hydration. As the hydration proceeded, the quantity of  $Q_2$  species produced increased, indicating an increase in the average chain length of the product C-S-H gel. There was a small overlap between the  $Q_1$  and  $Q_2$  resonances. The line widths of the  $Q_1$  and  $Q_2$  resonances were found to be largely independent of the temperature, with the exception that the line width of the  $Q_1$  resonance was marginally increased at the highest temperature studied. The peak intensities of the isotropic peaks and the first-order spinning sidebands in these spectra were integrated, and corrections were performed to allow for the effects of partial saturation of the NMR resonances, and for the intensity contained in the second-order spinning sidebands which were not included in the integration. The results are plotted on a logarithmic time scale in Fig. 2 and plotted for the degree of hydration (as measured by NMR) in Fig. 3. Fig. 4 shows plots of the chain length plotted with respect to the degree of hydration for all three temperatures. Note that at the higher temperatures, no data was available for low degrees of hydration, because the rapid hydration gave rise to very limited periods of time in which to acquire the spectra.

### 3.2. $^{29}\text{Si}$ CPMAS NMR spectra

At intervals during the hydration of each sample,  $^{29}\text{Si}$  CPMAS NMR spectra were obtained in addition to the single-pulse spectra described above; representative CPMAS spectra are shown in Fig. 5. Up to four resonances can be observed in some of these spectra. The  $Q_1$  and  $Q_2$  resonances from the hydrated gel can be seen clearly at  $-79$  and  $-85$  p.p.m., respectively; but, in addition, in some of the spectra a sharp resonance is observable at approximately  $-82.5$  p.p.m., as is a broad  $Q_0^{(H)}$  resonance in the region from  $-70$  to  $-75$  p.p.m. it is difficult to determine an exact chemical shift for this broad resonance because of significant overlap with the much more intense  $Q_1$  resonance; an upfield shift of this species was observed with increasing hydration, possibly indicating a change in the  $Q_0^{(H)}$  environment. The intensities of the resonances in the CP spectra are not quantitatively related to the concentration of the species giving rise to them; this is clearly visible in the series of spectra shown in Fig. 6, where the relative intensities of the four resonances are shown to be strongly dependent on the contact time. In particular the sharp resonance at  $-82.5$  p.p.m. became increasingly prominent at longer contact times. The observed intensities could not be fitted to the simple double-exponential model expected for species with single proton spin-lattice relaxation time in the rotating frame ( $T_{1\rho}$ ) and  $^1\text{H}$ - $^{29}\text{Si}$  cross polarization relaxation time ( $T_{\text{HSi}}$ ) values. It was possible,

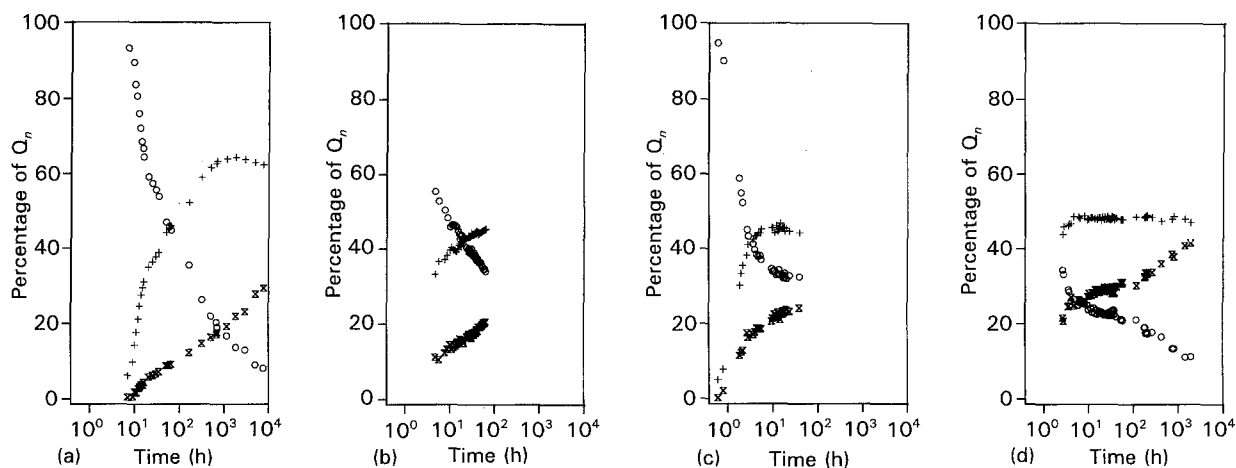


Figure 2  $Q_n$  values for  $C_3S$  hydration plotted with respect to a logarithmic time scale at temperatures of: (a) 20 °C, (b) 50 °C; (c) 75 °C, for a sample which was subjected to MAS at a very early degree of hydration, and (d) 75 °C, for two separate samples subjected to MAS at a later degree of hydration. (○)  $Q_0$ , (+)  $Q_1$ , and (x)  $Q_2$ . Data from a second sample run at 20 °C were extremely noisy, because of problems experienced with the spectrometer; they are not plotted here, but were similar in form to the run shown in Fig. 2a; only the data shown here are used in the rest of this paper. The first point in these graphs represents the stage at which these samples were subjected to MAS.

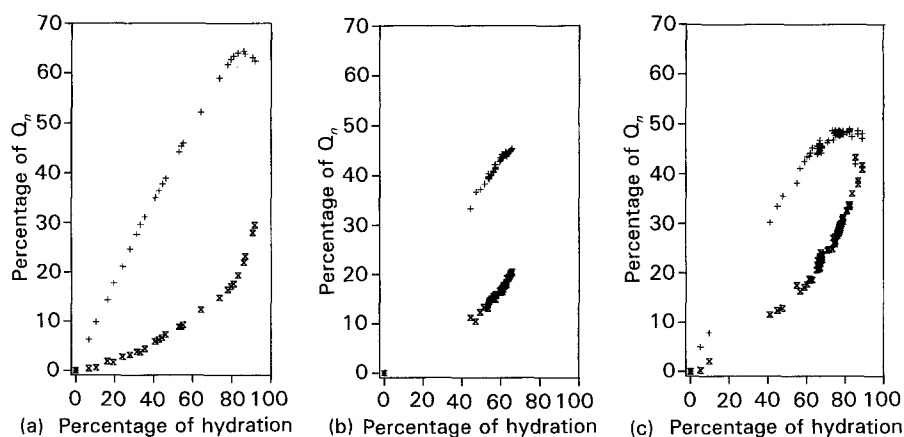


Figure 3  $Q_n$  values for  $C_3S$  hydration plotted for (+)  $Q_1$  and (x)  $Q_2$  with respect to the degree of hydration (calculated from NMR, as the percentage of silicate units no longer remaining as  $Q_0$  species) at temperatures of: (a) 20 °C, (b) 50 °C, and (c) 75 °C. The data from all three samples hydrated at 75 °C are superimposed, whereas data from only one experimental run is shown for each of the two lower temperatures.

however, to determine that the  $Q_0^{(H)}$ ,  $Q_1$  and  $Q_2$  resonance had similar relaxation parameters, while  $T_{1\rho}$  for the peak at  $-82.5$  p.p.m. was considerably longer. We attempted to quantify these CP spectra by calibrating their peaks relative to the peaks in the single-pulse spectra. Deconvolution of the CP spectra enabled the intensity of the  $Q_0^{(H)}$  resonance to be estimated relative to the resonance of  $Q_1$ . Since the percentages of the  $Q_1$  and  $Q_2$  resonances were known from the single-pulse spectra, the absolute intensity of the  $Q_0^{(H)}$  resonance could be calculated. Fig. 7 shows estimates of the intensity of the  $Q_0^{(H)}$  resonance at 20 °C and at 75 °C plotted with respect to the percentage of hydration. The degree of preferential excitement in the CP spectra, resulting from differences in the relaxation and cross relaxation rates of the species involved, is not known precisely. Hence, the intensity scale is not absolute.

### 3.3. Effects of quenching and MAS

In order to determine the effects of quenching, one of the samples was quenched by addition of propan-2-ol,

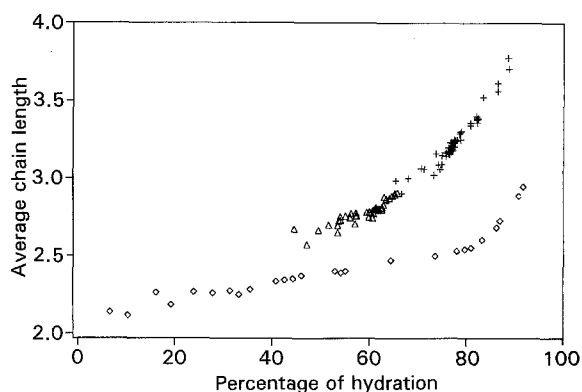


Figure 4 Average chain lengths for  $C_3S$  hydration temperatures plotted with respect to the degree of hydration at temperatures of: (+) 75 °C, ( $\Delta$ ) 50 °C, and ( $\diamond$ ) 20 °C. The average chain length was calculated as  $2 + 2(Q_2/Q_1)$ .

followed by outgassing under vacuum. Spectra were then taken of this sample; these spectra are compared in Fig. 8 with the spectra taken before quenching. It can be seen that the MAS spectra are essentially unchanged, which indicates that there is no detectable

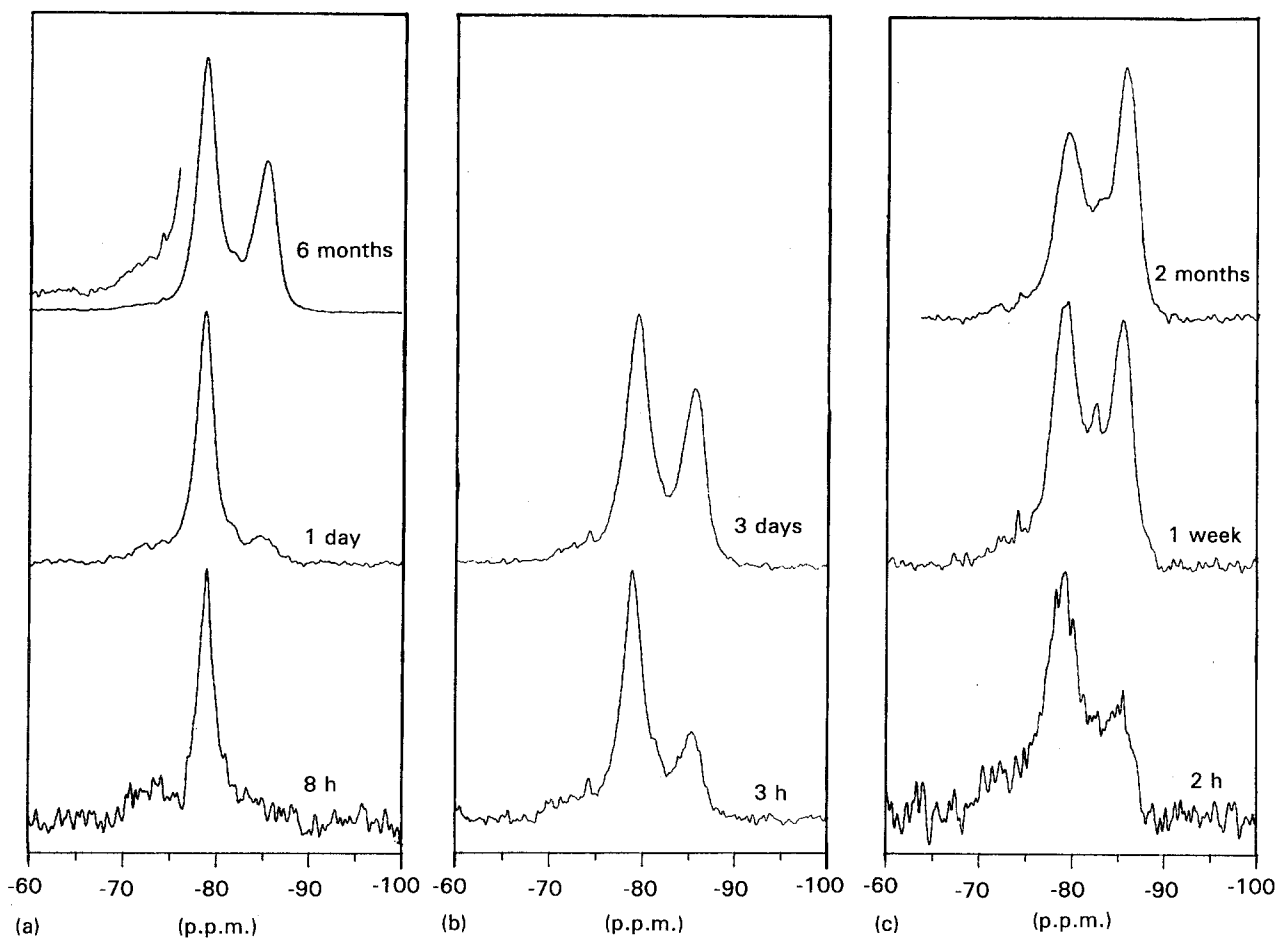


Figure 5 Representative  $^{29}\text{Si}$  CPMAS NMR spectra of  $\text{C}_3\text{S}$  samples hydrated at a water-to-solids ratio of 0.5 and temperatures of: (a)  $20^\circ\text{C}$ , (b)  $50^\circ\text{C}$ , and (c)  $75^\circ\text{C}$ . The isotropic peaks are labelled with the  $Q_n$  assignments. Only a very small fraction of the total number of spectra acquired from each sample are shown here.

change in the silicate polymerization. There are some changes of up to about 10% in the relative intensities of the peaks in the CPMAS spectra, but these can be attributed to changes in the proton mobility, and hence to changes in the parameters  $T_{\text{HSi}}$  and  $T_{1\rho}$ , which determine the intensities observed in the CP spectra, rather than a change in the relative intensities of the species in the spectra (the additional peak at  $-82.5$  p.p.m. that appeared in both the quenched and the real time  $^{29}\text{Si}$  CP spectra is discussed elsewhere in this paper).

Fig. 9 shows the results of an experiment designed to determine the effects of MAS upon the hydration of  $\text{C}_3\text{S}$ . Two samples of  $\text{C}_3\text{S}$  were hydrated at approximately  $75^\circ\text{C}$  for 18 h. One sample was hydrated in a static container in an oven at  $80^\circ\text{C}$ ; the other sample was hydrated while being subjected to MAS, at a temperature of approximately  $75^\circ\text{C}$ . The MAS NMR spectra run subsequently were essentially the same for the material hydrated for the same period of time, with and without MAS, although the degree of hydration was somewhat greater for the sample hydrated under static conditions; this was probably a result of this sample experiencing a slightly higher temperature during hydration. In contrast, the CPMAS NMR spectra differed significantly, with an additional peak occurring at  $-82.5$  p.p.m. in the spectrum of the sample that was subjected to MAS. From the single-

pulse spectra, it would appear that this species only formed a few per cent of the total hydration products.

### 3.4. Two-dimensional $^{29}\text{Si}$ NMR spectra

Since the samples studied in this paper were enriched in  $^{29}\text{Si}$  to 100%,  $^{29}\text{Si}$ - $^{29}\text{Si}$  dipolar and scalar couplings will have existed in the C-S-H gel, and it should be possible in principle to utilize these couplings to determine the bonding between the different silicate species. Attempts to obtain  $^{29}\text{Si}$  correlation spectroscopy (COSY) spectra did not result in any observation of significant cross peaks; the line widths were too large for this pulse sequence to be successful. The COSY sequence works via the scalar couplings, and so it would have provided direct evidence of through-bond  $^{29}\text{Si}$ -O- $^{29}\text{Si}$  connectivities. We were able, however, to obtain  $^{29}\text{Si}$  nuclear Overhauser effect spectroscopy (NOESY) spectra using the standard pulse sequence [33] (but with CP excitation). A typical spectrum is shown in Fig. 10. The horizontal scale represents the chemical shift experienced during the evolution time, while the vertical scale represents the chemical shift experienced during the acquisition time. Two types of peak can be observed; one type lies upon the diagonal, while the other type does not.

Peaks that lie upon the diagonal have the same chemical shift upon each axis; they represent magnetization initially located upon a given species, which

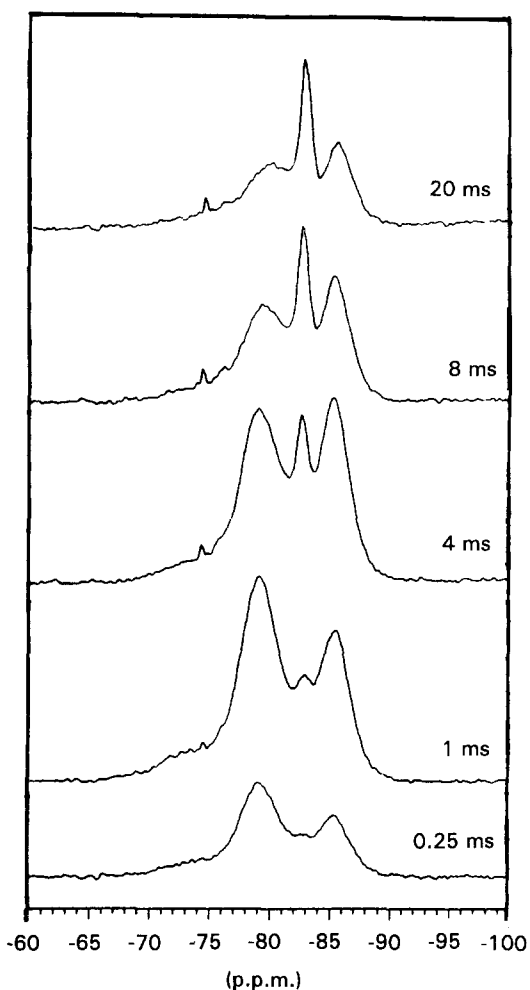


Figure 6 Variable-contact-time  $^{29}\text{Si}$  CPMAS NMR spectra of a sample of  $\text{C}_3\text{S}$  hydrated at  $75^\circ\text{C}$  for 18 h, and quenched with propan-2-ol, as described in the text.

remained upon that species throughout the experiment, experiencing the same chemical shift in both the evolution and the acquisition times. The off-diagonal or cross peaks represent magnetization that experienced different environments in the evolution and acquisition time, and hence that experienced different chemical shifts during those two periods. This is magnetization that was transferred from one resonance to another during the mixing time. The mixing process occurs through space for the NOESY experiment, and so long mixing times are required. The spin-diffusion process responsible for the transfer of magnetization is complex, and it does not have a simple distance dependence. Hence cross peaks in NOESY spectra are not direct evidence of  $^{29}\text{Si}-\text{O}-^{29}\text{Si}$  connectivities; they do indicate however that the species are close together on a nanometre scale, and hence they are within the same phase. The observation of cross peaks between the  $Q_1$  and  $Q_2$  resonances indicates that magnetization was transferred between these species during the mixing time, and that they must therefore be located within the same phase. There is no evidence for the species giving rise to the  $-82.5$  p.p.m. resonance being in this phase, since no cross peaks were observed involving this resonance.

### 3.5. TEM

A sample of  $\text{C}_3\text{S}$ , not enriched in  $^{29}\text{Si}$ , hydrated at  $80^\circ\text{C}$  for 1 day, was studied by TEM using techniques described previously in [10]. A TEM micrograph is shown in Fig. 11; the morphology is similar to that found in samples of  $\text{C}_3\text{S}$  hydrated at room temperature, but with a more open and coarse structure. Energy dispersive X-ray analyses were performed in the TEM, and they indicated a Ca:Si ratio of  $1.77 \pm 0.22$  (8 analyses) for the outer product, and  $1.72 \pm 0.13$  (15 analyses) for the inner product; these ratios are similar to those obtained previously for materials

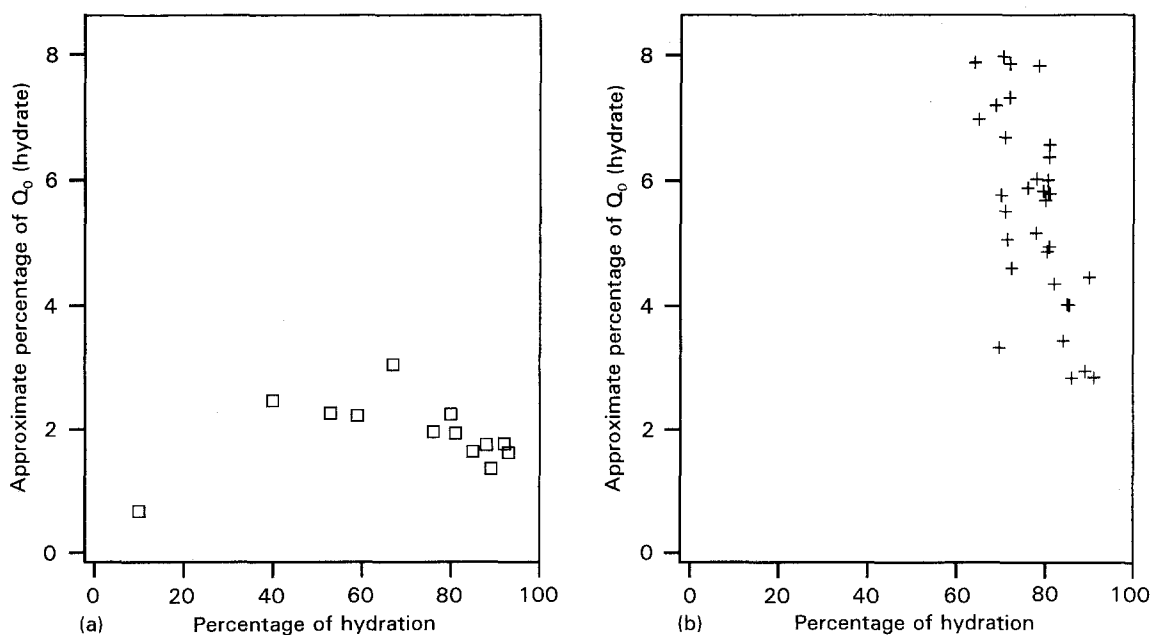


Figure 7 Estimates of the intensity of the  $Q_6^{(H)}$  resonance for samples of  $\text{C}_3\text{S}$  plotted with respect to the degree of hydration at hydration temperatures of: (a)  $20^\circ\text{C}$ , and (b)  $75^\circ\text{C}$ . The data for all three independent samples are superimposed in (b).

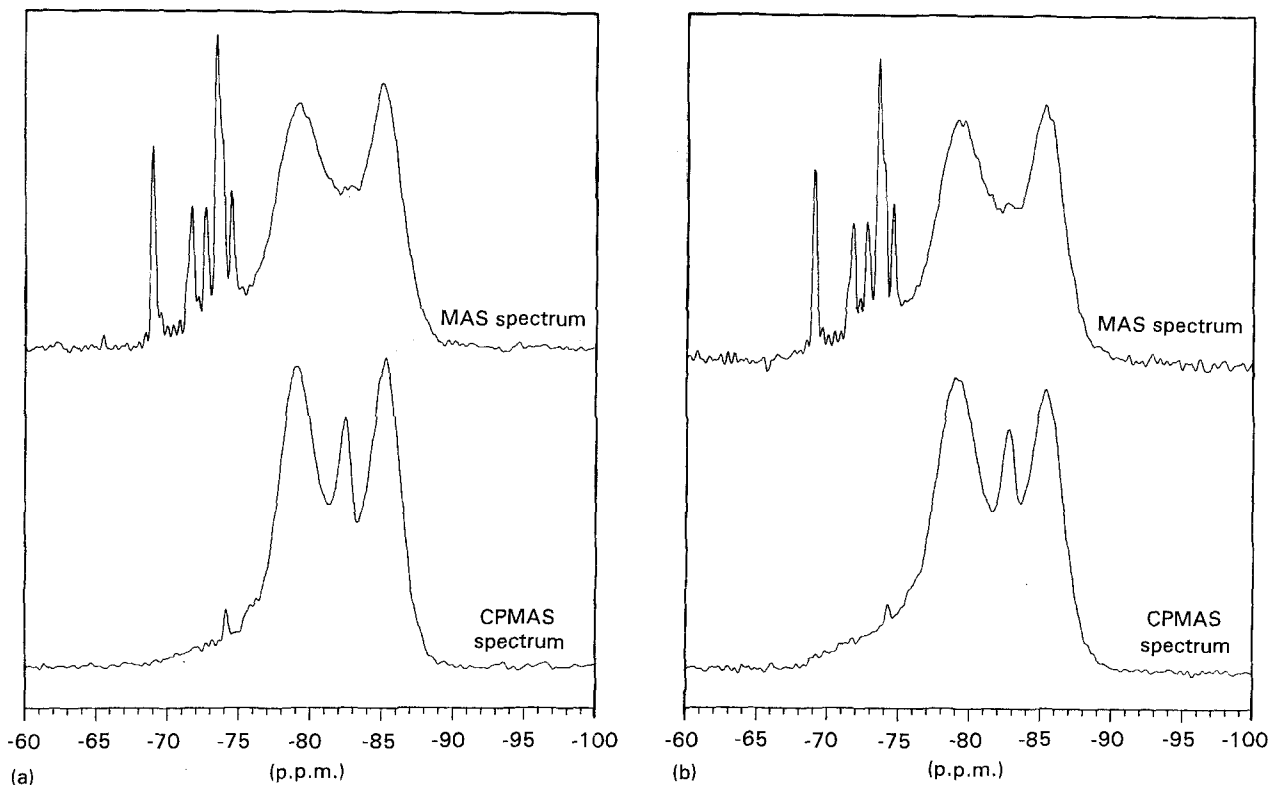


Figure 8 The effects of quenching.  $^{29}\text{Si}$  MAS and CPMAS spectra are shown for a sample of  $\text{C}_3\text{S}$  hydrated at  $75^\circ\text{C}$  for 18 h. The spectra were taken (a) before and (b) after quenching with propan-2-ol (isopropanol).

hydrated at room temperature. This sample of  $\text{C}_3\text{S}$  hydrated at  $80^\circ\text{C}$  was found to have a very low strength, and it crumbled during sectioning.

#### 4. Discussion

In this paper, we used *in-situ* or real-time  $^{29}\text{Si}$  MAS and CPMAS NMR to gather a large quantity of data relating to the hydration of  $\text{C}_3\text{S}$  over a wide range of temperatures. In this section, we will first assess the strengths and limitations of the approach used here, and then consider the chemical implications of the data which was acquired.

##### 4.1. Techniques

The samples were subjected to large forces as a result of the MAS technique, which was used in this study to obtain well-resolved NMR spectra very rapidly. We found that, in a number of experiments performed under these conditions, a small quantity of a species with distinct CP and relaxation properties was formed; this species was not seen in control samples. This species resonates at approximately  $-82.5$  p.p.m. and it is preferentially excited in CP spectra with long contact times; it is coupled to protons which have a  $T_{1\rho}$  value much longer than that for the  $\text{Q}_1$  and  $\text{Q}_2$  species in the sample. In the two-dimensional NOESY spectrum, cross peaks were not observed between the resonance at approximately  $-82.5$  p.p.m. and those due to the normal  $\text{Q}_1$  and  $\text{Q}_2$  species; this suggests that the species is in a different phase from the bulk of the sample. It is possible that this phase results from precipitation of hydrate from the small quantities of

bleed water that might be expected to result from the large centrifugal forces induced by the MAS technique. The crystalline phase tri-calcium-silicate hydrate has previously been observed to resonate at a similar shift [34]. The quantity of the new species formed was small ( $< 5\%$ ), with no distinct observable peak within the single-pulse spectra. The relative intensities of the resonances from the major hydration products were not affected; similar single-pulse spectra were obtained from samples hydrated in an oven and in the NMR probe at a similar elevated temperature, under the MAS conditions; see Fig. 9. The degree of hydration of these two samples differed slightly, as expected, since they were not hydrated at exactly the same temperature ( $80^\circ\text{C}$  and  $75^\circ\text{C}$ ). The course of the hydration reaction of  $\text{C}_3\text{S}$  as observed by real-time  $^{29}\text{Si}$  NMR of  $^{29}\text{Si}$ -enriched samples, appeared to be broadly similar to the reaction observed in samples of  $\text{C}_3\text{S}$  hydrated under static conditions at room temperature, and at elevated temperature, and to be similar to the reactions reported in [13, 20, 35]. Clearly,  $^{29}\text{Si}$  MAS NMR spectra acquired *without quenching* will correctly identify the  $\text{Q}_n$  species present within a hydrating sample. Most of the results reported in the literature were acquired from *quenched* samples, and so it is important to assess the effects of quenching if the results are to be related to the results reported previously. The limited experiments reported in this paper suggest that *rapid* quenching with propan-2-ol has no effect upon the degree of polymerization of calcium-silicate-hydrate gels. This is in contrast to the behaviour previously reported for fresh gels, where the polymerization was found to depend upon the humidity during storage [19]. Changes in the CP spectra



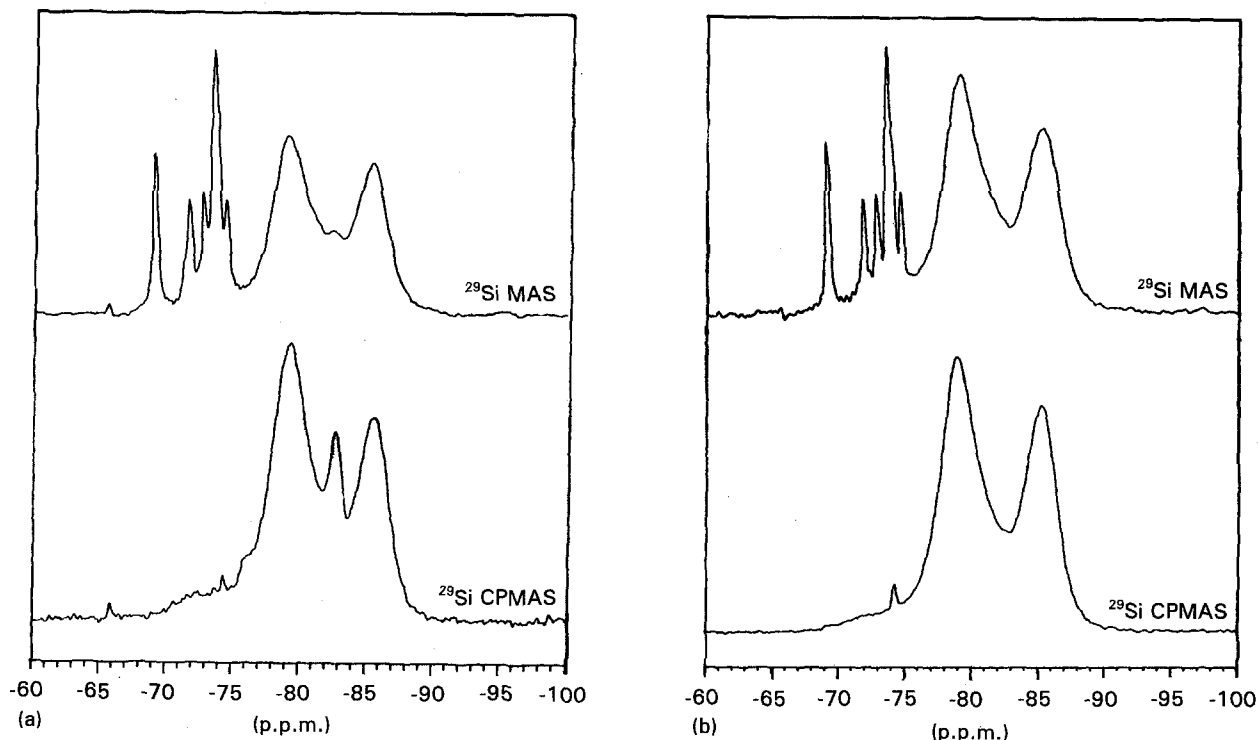


Figure 9 The effects of MAS.  $^{29}\text{Si}$  MAS and CPMAS spectra are shown for two samples of  $\text{C}_3\text{S}$  hydrated for 18 h. (a) The sample was hydrated at  $75^\circ\text{C}$  and subjected to MAS at 2 kHz after 2 h. (b) The sample was hydrated under static conditions at  $80^\circ\text{C}$  for the whole 18 h, and it was only then subjected to MAS.

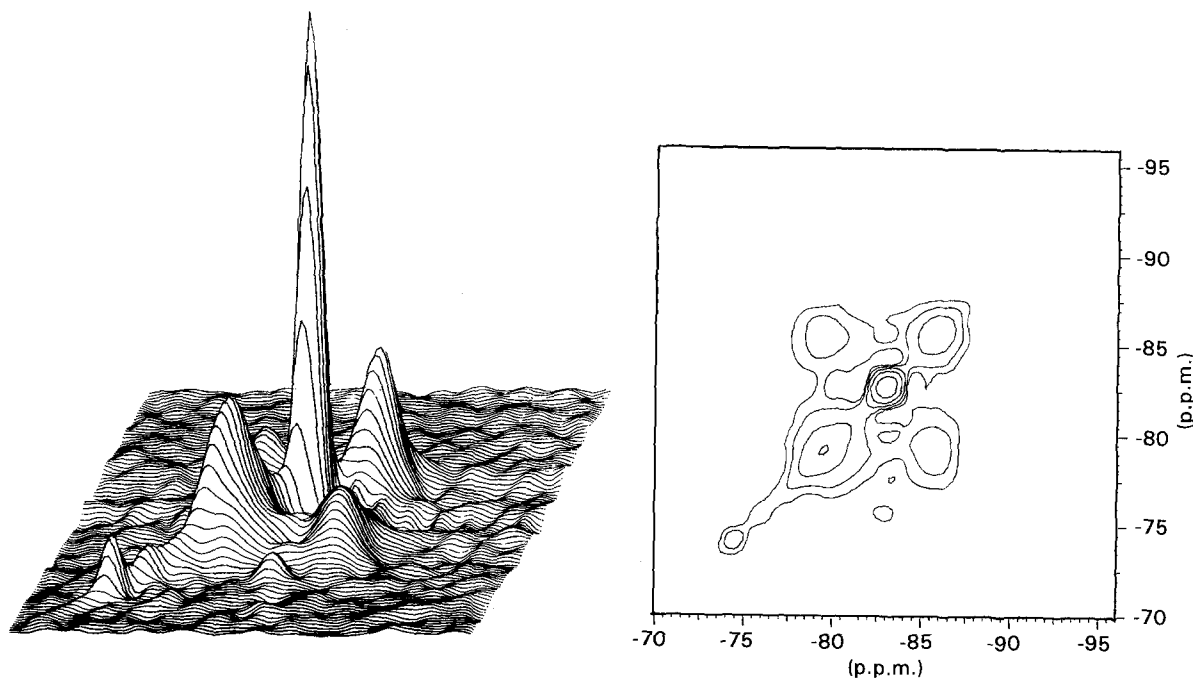


Figure 10 A  $^{29}\text{Si}$  CPMAS NOESY two-dimensional NMR spectrum of calcium-silicate hydrate, acquired from a sample of  $\text{C}_3\text{S}$  hydrated for 18 h at  $75^\circ\text{C}$  and subjected to MAS after 2 h; one-dimensional MAS and CPMAS spectra are shown for this sample in Fig. 8b. A mixing time of 5 s was used, MAS was performed at 2 kHz, and the excitation was performed by cross polarization with a contact time of 4 ms. 128 experiments were performed, with a sweep width in both dimensions after a transformation of 2500 Hz. The spectrum was acquired from a quenched sample at room temperature by MAS at 2 kHz.

upon quenching suggest, however, that the mobility of the protons is altered. Our results suggest that while the structure of the C-S-H gel may be significantly altered, no major reorganization of the *silicate-anion structure* takes place upon rapid quenching. It is not possible to determine the location of  $\text{Q}_0^{(\text{H})}$  species by NMR of quenched samples, since if this species were to be present in solution it would be precipitated by

the quenching process. This peak was observed in CP spectra acquired from unquenched samples, which indicates that it does not result from monomeric species in solution; solution species were not detected by CP excitation.

By the use of real-time hydration, we were able to acquire large amounts of data very rapidly from a single sample. Similar results could be obtained from

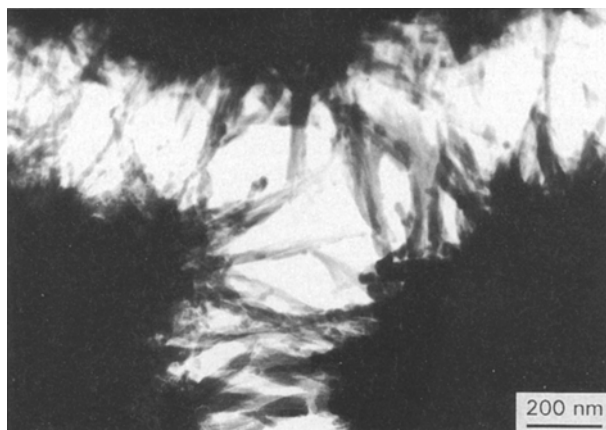


Figure 11 A TEM micrograph of unenriched  $C_3S$ , hydrated at  $80^\circ C$ , showing a coarse, fibrillar, outer product.

quenched  $^{29}Si$ -enriched samples, but such an approach is difficult and costly, because of the need repeatedly to recycle the  $^{29}Si$ , with consequent incremental losses and contamination of the  $^{29}Si$ -enriched material. With the use of unenriched silicates, it takes a time of the order of 24 h to obtain CP spectra with sufficiently good signal-to-noise ratios for the quantification of the approximately 2% of signal found for the  $Q_0^{(H)}$  resonance at room temperature. In contrast, such a spectrum may be obtained in 3 h or less by the use of  $^{29}Si$ -enriched material, even with the use of smaller samples sealed in rotor inserts. Similar arguments apply for the single-pulse data. The spectra shown in Figs 1 and 5 were not selected so as to have abnormally good signal-to-noise ratios, but they contained significantly less noise than many spectra presented in the literature. Many spectra of this quality can be obtained from a single sample, in a continuous experimental session. Such data have made it possible to determine changes in the average polymer chain length with far more certainty than has previously been the case. The work involved in quenching multiple samples is also avoided.

A potential difficulty with real-time spectral acquisition is water loss under the conditions of MAS; the steps taken to avoid this are described in the experimental section of this paper. Additionally, in many designs of commercially available double-bearing MAS NMR probes, some uncertainty in the temperature of the sample arises because the bearing gas is only regulated by a thermocouple which is well-separated from the sample to avoid shimming problems.

In the two-dimensional experiment, the cross peaks depend upon the transfer of magnetization from one  $^{29}Si$  nucleus to another. In an unenriched sample, 95% of such possible interactions would not occur, because of the presence of  $^{28}Si$  nuclei. The need for a long mixing time in this experiment results in loss of the signal, and also in a low-signal-to-noise ratio. Hence this experiment would not be viable with an unenriched sample. Two-dimensional experiments have been performed upon zeolites [36] with natural-abundance samples; very careful crystallization of the

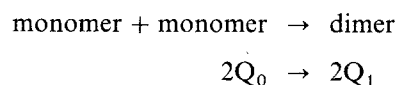
samples was required in order to give exceptionally narrow line widths and to enable use of the COSY experiment. This experiment did not include a mixing time, and so it had an inherently higher signal-to-noise ratio than the NOESY experiment. Although the large line widths exhibited by samples of C-S-H make use of the COSY experiment impractical, information can be obtained from NOESY experiments.

#### 4.2. Chemical implications of the data

The present results confirm previous suggestions [14] that the relative intensities of the various  $Q_0$  resonances are invariant throughout the course of the hydration reaction, and they indicate that dissolution of the silicate anions from  $C_3S$  is approximately congruent. There would appear to be no broadening of the  $Q_0$  peaks of  $C_3S$ , in contrast to the results obtained recently for  $\beta$ - $C_2S$  [37], implying that dissolution of the calcium ions is also congruent, and that the  $C_3S$  does not react in significant quantities with the water prior to dissolution, other than to form small quantities of the  $Q_0^{(H)}$  species.

The kinetics of the reaction correspond approximately to results obtained previously [16, 20, 21, 23, 24, 34, 35], both in terms of the rate and the distribution of the products. At all three temperatures studied, a maximum rate was reached at quite an early stage of the reaction, and the reaction rate decreased continuously thereafter. This suggests that the hydration reaction speeds up as the conditions either for dissolution of  $C_3S$  or for precipitation of the products become more favourable. Once products start to be produced in quantity, the products physically block the course of the reaction, and this results in the continuous reduction in the rate. This reduction in the rate is found to be more abrupt at the later stages of the reaction than would be expected on the basis of the Avrami equations [25], which may be fitted to the early stages of the reaction for a reaction order of 2.5.

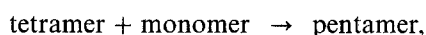
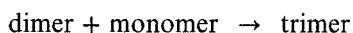
We will now consider the changes in the proportions of the various  $Q_n$  species in the hydrating system, and the potential for discriminating between various mechanisms of the hydration reaction on the basis of these proportions. It is found that hydration appears to take place in two stages; in the first stage, dimerization occurs, and then at later stages of the reaction polymerization occurs, probably by linking of the dimers with monomers to form longer chains. We start by considering the changes in polymerization of the silicate anions that would result from three possible model reaction schemes. In all these model schemes, the initial reaction is of two monomers to form a single dimer (possibly via an intermediate hydrated monomeric species) which can be written



The second stage of the reaction, corresponding to growth of the chains, could then proceed in a number of ways.

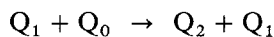
*Scheme 1* Polymerization could take place by linear

addition of monomers to the end of the growing chain

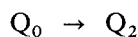


etc.

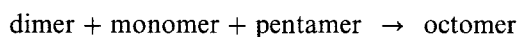
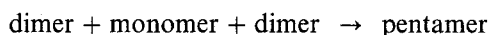
This is equivalent to the reaction



or, overall, to

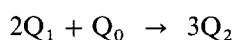


*Scheme II* Dimers, or longer chains could be linked together by monomers to form longer units

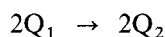
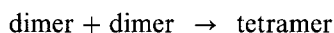


etc.

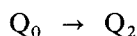
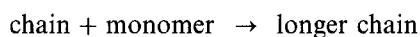
Or in terms of  $Q_n$  units



*Scheme III* The ongoing reaction could proceed by linking of species at random. This can lead to two possible reactions, chain linking,



or monomer addition to the end of a chain



Given the stoichiometry of the reactions for each scheme, it is possible to calculate the maximum chain length that can be achieved at 100% hydration with each model, given the proportions of species present at the longest hydration times studied in this paper (Table I). Take Scheme I as an example at 20°C. Under Scheme I,  $Q_0 \rightarrow Q_1$  is the only possible reaction, hence the  $Q_1$  species present at the end of the time period studied will be expected to persist until the completion of the hydration. Since at 92% hydration we observed that there were 62% of the  $Q_1$  species, then we must have at least 62% of the  $Q_1$  species at the completion of the hydration; the rest of the  $Q_0$  species could be converted into  $Q_2$  species, giving up to 38% of  $Q_2$  at complete hydration. This corresponds to an average chain length at the completion of the hydration of approximately 3.1. The results of equivalent calculations for each of the suggested polymerization schemes are summarized in Table II for the temperatures 20°C and 75°C. These maximum chain

TABLE I Proportions of the various  $Q_n$  species present at the upper limits of hydration; the data were obtained from Fig. 2

Temperature (°C)	$Q_0$	$Q_1$	$Q_2$
20	0.08	0.62	0.30
75	0.10	0.42	0.48

TABLE II The maximum chain lengths that could be reached on the basis of the reaction schemes I–III, given completion of the hydration reaction according to the reaction schemes shown for the samples reported in Table I; the calculations assume that all the remaining monomers react by the scheme shown, and did not undergo dimerization (Max.  $Q_2$  indicates the maximum proportion of  $Q_2$ , at the completion of hydration, that can be generated by this process; Max. CL indicates the maximum chain length that can similarly be reached)

Scheme	Process	20 °C		75 °C	
		Max. $Q_2$	Max. CL	Max. $Q_2$	Max. CL
I	$Q_0 \rightarrow Q_2$	0.38	3.1	0.58	4.8
II	$2Q_1 + Q_0 \rightarrow 3Q_2$	0.54	4.2	0.78	9
III	$Q_0 \rightarrow Q_2$	1.00	$\infty$	1.00	$\infty$
	$2Q_1 \rightarrow 2Q_2$				

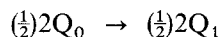
lengths were calculated from the proportions of the various  $Q_n$  species present at the longest hydration times studied in this paper (Table I).

Previous studies of old samples of hydrated  $C_3S$  at 20°C suggest a final chain length of approximately 4.5 [38]. A similar figure is achieved by the 140-year-old sample of Aspin's Portland cement [19], although the history of this sample is rather unusual. Scheme I does not allow for sufficient polymerization to reach these observed chain lengths. In addition, for the data acquired at 20°C, the quantity of the  $Q_1$  species appears to reach a maximum and then to fall; this rules out Scheme I, in which the intensity of the  $Q_1$  resonance can only rise. The fall in  $Q_1$  is only small, however, and it could possibly result from inaccuracies in the calibration of the intensities in these spectra. Schemes II or III do generate sufficient polymerization of the samples to attain the chain lengths at 100% hydration which have been previously reported in the literature. Scheme III, however, is likely to result in the growth of the chains to lengths well in excess of those actually observed experimentally in fully hydrated samples. It is, of course, possible that polymerization could take place by a combination of the suggested routes, rather than by a single process.

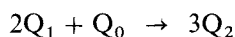
We shall consider Scheme II in more detail now, since this scheme appears to result in polymerization up to the chain lengths observed for very old samples in which hydration is essentially complete [19, 38], and also to fit a dreierketten-type model for the structure of C–S–H, as has been previously suggested [1, 2, 3]. We eliminate Schemes I and III, which do not fit with these structural models, and where extrapolation of our results to the completion of hydration would not appear to give chain lengths in agreement with those observed previously.

It is possible to utilize our model (Scheme II), and to calculate from the observed proportion of the  $Q_n$  species the proportions of monomeric silicate units which react to form dimers, or which form links between chain-end groups resulting in polymerization. Assume that for every monomer that undergoes dimerization,  $x$  monomers undergo the polymerization reaction. Then in a time  $\delta t$ , if  $\delta y$  monomers react to

form dimers



then in the same time  $\delta t$ ,  $x\delta y$  monomers will take part in the polymerization reaction



Thus in a time  $\delta t$ , the intensities  $I_n$  of the  $Q_n$  resonances will change as follows

$$I_0 \rightarrow I_0 - (1 + x)\delta y$$

$$I_1 \rightarrow I_1 + (1 - 2x)\delta y$$

$$I_2 \rightarrow I_2 + 3x\delta y$$

And in the limit as  $\delta t \rightarrow 0$

$$\frac{dI_0}{dt} = -(1 + x)\frac{dy}{dt}$$

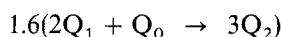
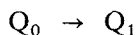
$$\frac{dI_1}{dt} = +(1 - 2x)\frac{dy}{dt}$$

$$\frac{dI_2}{dt} = +3x\frac{dy}{dt}$$

By measuring the changes of the intensity of the various  $Q_n$  species with respect to time, the term  $dy/dt$  can be eliminated, and then the equations can be solved for  $x$ . For example, for hydration at 20°C, at 92% hydration, from Fig. 3

$$\frac{dI_2/dt}{dI_1/dt} = -2.2 = \frac{3x}{1 - 2x}$$

Giving  $x = 1.6$ ; that is, the following reactions occur



In practice, although the noise in the  $I_1$  and  $I_2$  data is small it makes it difficult to calculate instantaneous rates, since plots of these data against the time or degree of hydration both follow curves with quite rapid changes of gradient. Instead, it was easier to work from the gradient of the chain-length curve,  $dL/dh$ , which is approximately linear for much of the

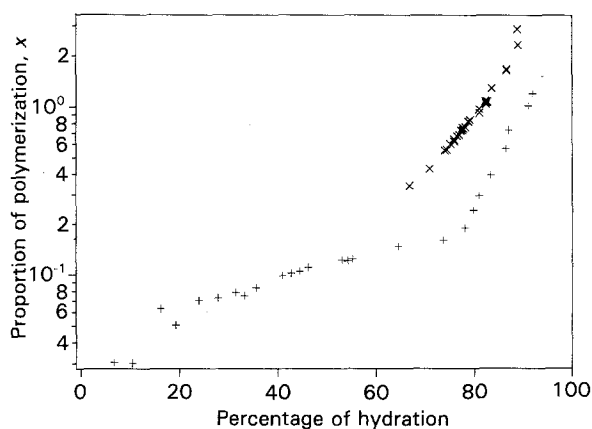


Figure 12 The variation of  $x$  with respect to the percentage of hydration for  $C_3S$  samples hydrated at: (+) 20°C, and (x) 75°C.  $x$  represents the number of monomeric silicate units which react to link together existing chains, relative to those that simply dimerize.

course of hydration (see Fig. 4). Then

$$x = \frac{2I_2 + I_1^2 dL/dh}{6I_1 - 4I_2 - I_2^2 dL/dh}$$

Fig. 12 shows plots of the value of  $x$  for the ranges of hydration studied at 20 and 75°C. The data at 75°C only cover a limited hydration range; data at lower degrees of hydration were too noisy for useful analysis. As might be expected,  $x$  increased throughout the course of the hydration reaction; at room temperature, nearly all of the monomers were initially converted to dimers ( $x \approx 0.02$ ), while by the limit of the acquired data, polymerization had become significant. Extrapolation of the chain length plot for hydration at 20°C to zero hydration gives an initial chain length of approximately 2.1; this corresponds to 5% of the hydrate being in  $Q_2$  units. Thus, initially,  $I_2 = 0.05I_1$  and we can solve for  $x$  using

$$x = \frac{2 \times 0.05I_1 + I_1^2 \times 2.1}{6I_1 - 4 \times 0.05I_1 - 0.05^2 I_1^2 \times 2.1}$$

$$= \frac{0.1 + 4.2I_1}{6 - 0.2 - 0.00525I_1}$$

In the limit as  $I_1 \rightarrow 0$  (zero hydration),  $x = 0.018$ ; that is one monomer undergoes polymerization for approximately every 50 which react to form dimers: polymerization is an insignificant process at this stage of the hydration reaction. It can be seen, from Fig. 12, however, that at later stages of the hydration reaction  $x$  increases and polymerization becomes a significant reaction. It would appear that reaction at early stages of hydration predominantly involves the dimerization of monomeric units to form dimers, but that significant polymerization occurs at later stages of hydration. The rate of this polymerization reaction corresponds to the formation of  $Q_2$  species. We shall now consider the temperature dependence of these two reactions. Suppose that for early stages of reaction  $I_1 = f(t/g(T))$ , then  $t/g(T) = f'(I_1)$ , since  $I_1$  is a monotonically decreasing function ( $I_1$  is the proportion of the  $Q_1$  resonance at time  $t$  and temperature  $T$ ).  $g(T)$  is the rate constant at temperature  $T$ . Then it follows that for the same value of  $I_1$  to be reached at different temperatures, the value of  $t/g(T)$ , and hence of  $\ln(t/g(T))$  ( $= \ln t - \ln g(T)$ ), must be constant. Hence a shift of  $\ln g(T)$  in the plot of  $I_1$  with respect to  $\ln t$  superimposes the values of  $I_1$  for the different temperatures. It can be seen in Fig. 13, where appropriate shifts in the  $\log t$  axis have been applied, that the overall changes in the rate of  $Q_1$  formation with time are similar for the three temperatures, at least if just the first 40% of hydration is considered. The limited data available at 50°C were not really sufficient to locate the offset for this curve accurately.

Suppose that the hydration reaction follows the Arrhenius function  $g(T) = g_0(T) \exp(-\Delta H/RT)$ , then  $\ln g(T) - \ln g_0(T) = \Delta H/RT$ , and the gradient of a graph of  $\ln g(T)$ , or equivalently of the logarithmic shifts  $\ln g(T) - \ln g(20^\circ\text{C})$ , plotted against  $1/T$  will yield a value for  $\Delta H$ .  $\ln g(T) - \ln g(20^\circ\text{C})$  is the logarithmic shift required in order to achieve overlap in Fig. 13. This calculation was performed with an Arr-

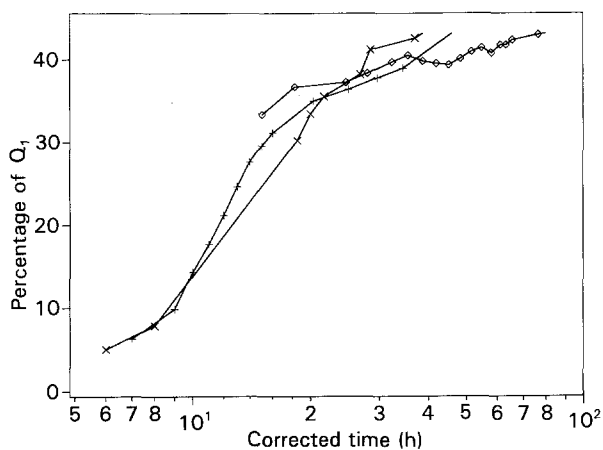


Figure 13 The close similarity between the kinetics of the first 50% of hydration of  $C_3S$  at ( $\times$ ) 20°C, ( $\diamond$ ) 50°C, and ( $+$ ) 75°C. The plots of the percentage  $Q_1$  are given with respect to logarithmic corrected times. The times shown are those for hydration at room temperature. The times for hydration at 50°C and 75°C were multiplied by factors of 3.2 and 10.0, respectively, to achieve alignment.

henius energy of  $35 \text{ kJ mol}^{-1}$  being found. The points deviate significantly from a linear plot, as expected, since the point at 50°C was determined on the basis of very limited data. Similar calculations can be performed for the formation of  $Q_2$  species at later stages in the hydration; the results are shown in Fig. 14, and analysis yields a value for the Arrhenius energy of  $100 \text{ kJ mol}^{-1}$  for this reaction. This value is more than twice that for the early stages of the reaction. The Arrhenius energies found in this work are broadly comparable to those reported previously [23, 24], but we were able to investigate specific stages of the reaction. It would appear, therefore, that at early stages of the hydration reaction dimerization is the predominant process, and it is characterized by a relatively low Arrhenius energy. At later stages of the reaction, linking of the dimeric units with monomers to form longer chains takes place, and this results in the generation of  $Q_2$  species; this process would appear to be characterized by a much larger Arrhenius energy, possibly because of the need to overcome not only the chemical activation energy but also the activation energy for diffusion of the  $Q_0$ -silicate species from the surface of the anhydrous  $C_3S$  grains to the reaction sites.

Fig. 7 shows the estimated percentages of  $Q_0^{(H)}$  present throughout the hydration reaction. A small upfield shift of the resonance was observed as the hydration increased; this possibly indicates a change in the environment of this species. It would appear that, once the end of the induction period is reached, the quantity of this species remains approximately constant at 2%, (at least up to 90% hydration) for the hydration process occurring at 20°C. It has been suggested previously [29] that this  $Q_0^{(H)}$  resonance may result from surface hydroxylation of  $C_3S$ . This  $Q_0^{(H)}$  species remain, however, at late stages of the hydration reaction, so it is unlikely that this is the case. Most of the small anhydrous particles will have become completely hydrated by the late stages of the hydration reaction; a very thick layer would be re-

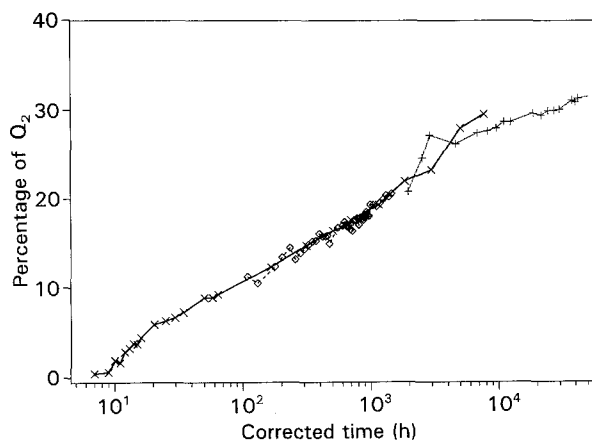


Figure 14 The close similarity between the kinetics of the formation of the  $Q_2$  species in the hydration of  $C_3S$  at ( $\times$ ) 20°C, ( $\diamond$ ) 50°C, and ( $+$ ) 75°C. The plots are given with respect to logarithmic corrected times. The times shown are those for hydration at room temperature. The times for hydration at 50°C and 75°C were multiplied by factors of 23 and 700, respectively, to achieve alignment.

quired upon the remaining anhydrous grains to account for the observed results. It would appear either that the  $Q_0^{(H)}$  species are in a separate phase, or that they represent mismatched  $Q_0$  species incorporated into defect sites in the dreierketten structure of the calcium-silicate-hydrate gel. There are greater quantities of monomeric silicate remaining at later stages of the hydration reaction at 75°C, and the  $Q_1$  resonance at the equivalent stage of reaction is distorted. Hydration, however, is more rapid at the higher temperature, and there would be less time for rearrangement of the silicate species upon the calcium-oxide layers of the structure, particularly as it would appear to be the polymerization reaction that is accelerated most at higher temperatures. Hence it is quite possible that rapid polymerization may be trapping monomeric species in defect sites in the dreierketten structure.

## 5. Conclusions

Use of  $^{29}\text{Si}$  enrichment and real-time acquisition in the study of the hydration of  $C_3S$  by  $^{29}\text{Si}$  MAS and CPMAS NMR allowed large quantities of high-quality data to be generated without the need for quenching of individual samples, and with only a limited demand for NMR spectrometer time. Series of data for hydration at 20, 50 and 75°C were acquired using this approach in order to investigate some aspects of the mechanism of hydration of  $C_3S$ . The basic features of hydration are unchanged by the MAS technique, despite the large forces that this imposes upon the hydrating gel. The only change observed was the production of a very small quantity of a hydrate (possibly tri-calcium-silicate hydrate) with a single  $^{29}\text{Si}$  resonance at a chemical shift of approximately  $-82.5 \text{ p.p.m.}$  Great care is, however, required in sealing the samples, in order to prevent water loss; also, the temperature calibration of commercial MAS NMR probes is rather crude, so that there is some uncertainty in the sample temperature. Importantly, the acquisition of  $^{29}\text{Si}$  spectra from samples hydrating

*in situ* in the NMR probe, without quenching, has made it possible to show that rapid quenching with propan-2-ol followed by vacuum outgassing does not detectably change the extent of silicate polymerization of the C-S-H gel.

After an induction period, hydration initially proceeded rapidly, but thereafter, the rate of the reaction decreased; the observed kinetics agreed with those obtained previously, both by NMR and by other techniques. The rate of reaction, and also the degree of silicate polymerization at a given degree of hydration were both significantly increased at elevated temperatures. At room temperature, extrapolation of a plot of chain length against hydration indicated that at early stages of hydration an average chain length of approximately 2.1 was found; the early hydrate is essentially dimeric material. Three potential models for the growth of chains were considered, and on the basis of the observed changes in the chain lengths it was possible to exclude the case (Scheme I) where chains grew incrementally (that is monomer → dimer → trimer → tetramer, etc.). On the basis of the chain length that could be reached at complete hydration, starting from the measured polymerization at the latest times studied in this paper, a model in which random fragments are linked (Scheme III) is also unlikely.

The linking of dimers with monomers (Scheme II), to form pentamers, octomers, etc, as has been postulated and observed previously [5, 6], is, however, consistent with the observed changes of silicate polymerization and with formation of a dreierketten structure. This would involve the linking of dimeric silicate species on a calcium-oxide layer, by reaction with monomers, to form a Tobermorite-type structure. Scheme II is also consistent with recent results obtained for a system with a high aluminium content, where dimeric silicate units appeared to be linked together by insertion of aluminate tetrahedra [39]. The proportion of monomers undergoing the polymerization linking reaction started at a very low value, and it increased throughout the hydration reaction, particularly after about 80% hydration. Dimerization, however, remained important, even at a 92% hydration. Arrhenius energies were determined for the temperature dependence of the two stages of reaction, early hydration produced  $Q_1$  species (dimers) ( $35 \text{ kJ mol}^{-1}$ ), and formation at later stages of the reaction produced  $Q_2$  species ( $100 \text{ kJ mol}^{-1}$ ). Finally, the use of real-time *in-situ* hydration with  $^{29}\text{Si}$ -enriched  $\text{C}_3\text{S}$  allowed the  $Q_0^{(H)}$  species to be quantified throughout the hydration reaction, rather than just during and shortly after the induction period.  $Q_0^{(H)}$  species persisted to late stages of the reaction, which indicates that they are unlikely to result from surface hydroxylation of  $\text{C}_3\text{S}$ . Instead, the  $Q_0^{(H)}$  species apparently result either from a distinct hydrate phase or from monomers present at defect sites in the dreierketten structure of the C-S-H gel. An upfield shift of this resonance with increasing hydration may indicate a change in the environment of the  $Q_0^{(H)}$  species. The amount of  $Q_0^{(H)}$  formed appears to be significantly increased at higher temperatures.

## Acknowledgements

We acknowledge the SERC for support under grant GR/H64972, and also for grants towards the purchase of NMR equipment and for provision of a studentship (for ARB). We thank the Inorganic Chemistry Laboratory workshops for machining supplies of rotor inserts, M. J. Seaman for writing C code to enable the conversion of 24-bit binary data from a Bruker MSL200 into formats suitable for general use, and S. J. Eyles for general assistance with computing.

## References

1. I. G. RICHARDSON and G. W. GROVES, *Cem. Concr. Res.* **22** (1992) 1001–1010.
2. H. F. W. TAYLOR, *J. Amer. Ceram. Soc.* **69** (1986) 464–467.
3. F. P. GLASSER, E. E. LACHOWSKI and D. E. MACPHEE, *ibid.* **70** (1987) 481–485.
4. A. M. DUNSTER, J. R. PARSONAGE and E. A. VIDGEON, *Mater. Sci. Technol.* **5** (1989) 708–713.
5. J. HIRLJAC, Z.-Q. WU and J. F. YOUNG, *Cem. Concr. Res.* **13** (1983) 877–886.
6. L. S. DENT-GLASSER, E. E. LACHOWSKI, M. Y. QURESHI, H. P. CALHOUN, D. J. EMBREE, W. D. JAMIESON and C. R. MASSON, *ibid.* **11** (1981) 775–780.
7. E. E. LACHOWSKI, *ibid.* **9** (1979) 337–342.
8. A. DUREKOVIĆ, *ibid.* **18** (1988) 532–538.
9. I. G. RICHARDSON and G. W. GROVES, *J. Mater. Sci.* **28** (1993) 265–277.
10. G. W. GROVES, P. J. LE SUEUR and W. SINCLAIR, *J. Amer. Ceram. Soc.* **69** (1986) 353–356.
11. A.-R. GRIMMER and F. VON LAMPE, *Z. Chem.* **23** (1983) 343–344.
12. E. LIPPMAA, M. MÄGI, A. SAMOSON, G. ENGLEHARDT and A.-R. GRIMMER, *J. Amer. Ceram. Soc.* **102** (1980) 4889–4893.
13. E. LIPPMAA, M. MÄGI and M. TARMAK, *Cem. and Concr. Res.* **12** (1982) 597–602.
14. N. J. CLAYDEN, C. M. DOBSON, C. J. HAYES and S. A. RODGER, *J. Chem. Soc., Chem. Comm.* **21** (1984) 1396–1397.
15. N. J. CLAYDEN, C. M. DOBSON, G. W. GROVES, C. J. HAYES and S. A. RODGER, *Proc. B Ceram. Soc.* **35** (1984) 55–64.
16. Y. TONG, H. DU and L. FEI, *Cem. Concr. Res.* **21** (1991) 355–358.
17. S. A. RODGER, D. Phil. thesis, University of Oxford, Oxford 1986.
18. H. F. W. TAYLOR and D. E. NEWBURY, *Cem. Concr. Res.* **14** (1984) 93–98.
19. D. E. MCPHEE, E. E. LACHOWSKI and F. P. GLASSER, *Adv. Cem. Res.* **1** (1988) 131–137.
20. S. MASSE, H. ZANNI, J. LECOURTIER, J. C. ROUSSEL and A. RIVEREAU, *Cem. Concr. Res.* **23** (1993) 1169–1177.
21. S. U. AL-DULAIJAN, G. PARRY-JONES, A. J. AL-TAYYIB and A. I. AL-MANA, *J. Amer. Ceram. Soc.* **71** (1990) 736–739.
22. G. PARRY-JONES, A. J. AL-TAYYIB and A. I. AL-MANA, *Cem. Concr. Res.* **18** (1988) 229–234.
23. P. FIERENS, Y. KAMUEMA and J. TIRLOCQ, *ibid.* **12** (1982) 191–198.
24. A. M. URZHENKO and A. V. USHEROV-MARSHAK, *Inorg. Mater.* **10** (1974) 761–764.
25. J. D. HANCOCK and J. H. SHARP, *J. Amer. Ceram. Soc.* **55** (1972) 74–77.
26. S. R. HARTMANN and E. L. HAHN, *Phys. Rev.* **128** (1962) 2042–2053.
27. C. S. YANNONI, *Acc. Chem. Res.* **15** (1982) 201–208.
28. S. A. RODGER, G. W. GROVES, N. J. CLAYDEN and C. M. DOBSON, *J. Amer. Ceram. Soc.* **71** (1988) 91–96.
29. R. RASSEM, H. ZANNI-THEVENEAU, C. VERNET, D. HEIDEMMANN, A.-R. GRIMMER, P. BARRET, A. NONAT, D. BERTRANDIE, and D. DAMIDOT, Proceedings of the 1st International Workshop on Hydration and Setting,

- Dijon, France, 3–5 July, 1991.
30. J. ROCHA and J. KLINOWSKI, *J. Magn. Reson.* **90** (1990) 567–568.
  31. C. P. GREY, A. K. CHEETHAM and C. M. DOBSON, *ibid.* **A 101** (1993) 299–306.
  32. WAVEMETRICS, IGOR, Lake Oswego, Oregon, 97035, USA, (1992).
  33. N. M. SZEVERENYI, M. J. SULLIVAN and G. E. MACIEL, *J. Magn. Reson.* **47** (1982) 462–475.
  34. G. M. M. BELL, J. BENSTEAD, F. P. GLASSER, E. E. LACHOWSKI, D. R. ROBERTS and M. J. TAYLOR, *Adv. Cem. Res* **3** (1990) 23–37.
  35. G. PARRY-JONES, A. J. AL-TAYYIB, S. U. AL-DULAIJAN and A. I. AL-MANA, *Cem. Concr. Res.* **19** (1989) 228–234.
  36. C. A. FYFE, H. GEIS and Y. FENG, *J. Amer. Chem. Soc.* **111** (1989) 7702–7707.
  37. X. CONG and R. J. KIRKPATRICK, *Cem. Concr. Res.* **23** (1993) 1065–1077.
  38. S. A. RODGER, G. W. GROVES, N. J. CLAYDEN and C. M. DOBSON, *Mater. Res. Symp. Proc.* **85** (1987) 13–20.
  39. I. G. RICHARDSON, A. R. BROUGH, R. BRYDSON, G. W. GROVES and C. M. DOBSON, *J. Amer. Ceram. Soc.* **76** (1993) 2285–2288.

*Received 16 November 1993  
and accepted 3 February 1994*